PIER C

(Received 16 July 2025, Accepted 29 August 2025, Scheduled 22 September 2025)

Research on Electromagnetic Scattering Characteristics of Complex Bodies Loaded with Metasurfaces

Linghui Qi[1], Fan Ding[2], Xiaofeng Zhou[1], Cicheng Wang[1], Yang Fu[1], Ruonan Zhao[1], Junyu Liang[1], and Helin Yang[1,*]

[1]*College of Physical Science and Technology, Central China Normal University, Wuhan 430000, China*
[2]*Hanjiang National Laboratory, Wuhan 430070, China*

ABSTRACT: This paper presents the design of an absorptive metasurface suitable for complex-shaped targets, achieving precise control over electromagnetic waves, which has been experimentally validated. The metasurface, with a design thickness of only 0.27 mm, maintains sufficient absorption properties under appropriate curvature conditions to ensure the stealth characteristics of the coated target. Through simulation and experimental validation, this study demonstrates the metasurface's strong resonance characteristics near 11.26 GHz and a reduction of approximately 3 dB in far-field radar cross section (RCS) simulation. The experimental test results are almost consistent with the simulation results, confirming the metasurface's effectiveness in reducing the RCS of actual complex models. The research findings provide strong technical support for the radar stealth research of targets.

1. INTRODUCTION

In recent decades, metasurface technology has gained widespread attention and rapid development [1–4] due to its ability to precisely control electromagnetic waves through simple geometric shape design and material selection [5–8]. It has been widely applied in the fields of electromagnetic stealth [9, 10], encryption [11, 12], imaging [13–16], and advanced communication systems [17, 18]. The ability of metasurfaces to manipulate electromagnetic waves stems from their unique sub-wavelength structure design, which can be equivalent to basic circuit components such as capacitors and inductors [19]. After careful design and optimization, the desired electromagnetic characteristics can be achieved within the ideal frequency band. Periodically arranged metasurfaces can achieve macro-control of electromagnetic waves. Since the characteristics of metasurfaces mainly come from geometric design and material structure, they are usually lightweight and thin, making them suitable for many applications sensitive to mass, such as flying targets, where the impact of the metasurface's mass on the normal operation of these scenarios can be neglected.

Radar stealth technology, also known as stealth technology or low detectability technology, refers to the reduction or elimination of a target's radar reflection signals through various means, thereby reducing the possibility of the target being detected and tracked by radar. This technology is particularly important in the aerospace field, where it is used to enhance the survivability and combat effectiveness of equipment such as aircraft, ships, and missiles. It mainly includes low-scattering shape technology, stealth material technology [20], plasma stealth technology [6], and active stealth technology. Low-scattering shape technology involves designing the shape of weapons to eliminate features that can produce electromagnetic wave reflection effects. Stealth material technology mainly involves coating the surface of weapons with electromagnetic wave absorbing materials, using as much transparent-wave-absorbing composite structural materials as possible instead of metal to form the shape of weapons. Plasma stealth technology uses plasma generators, sheets, or radioactive isotopes to produce a plasma cloud around the weapon, absorbing radar electromagnetic waves or changing their propagation direction. Active radar stealth technology mainly includes active cancellation, smart skin, adaptive impedance loading, low probability of intercept technology, etc.

At present, there are a lot of basic theoretical researches on electromagnetic calculation [21–28] and research works that use electromagnetic simulation software to perform electromagnetic calculations on bodies coated with metasurfaces [29–32]. The purpose of these studies is usually to improve simulation efficiency while ensuring accuracy, or to verify the radar cross section (RCS) reduction effects of certain metasurfaces through simulations. However, most of these studies remain at the simulation level, and there is a significant gap in the field of experimental validation. For complex shapes, the fitting of metasurfaces is a challenge during simulation and small-scale experimental testing. Currently, some studies propose using an equivalent method, which involves inverting to determine the relative permittivity and relative permeability of metamaterials, and then assigning these properties to a new material to replace the modeling of metasurfaces during simulation [33, 34].

This study designed an absorptive metasurface suitable for complex-shape targets. Due to its design thickness of only 0.27 mm, it can still maintain sufficient absorption properties

* Corresponding author: Helin Yang (emyang@ccnu.edu.cn).

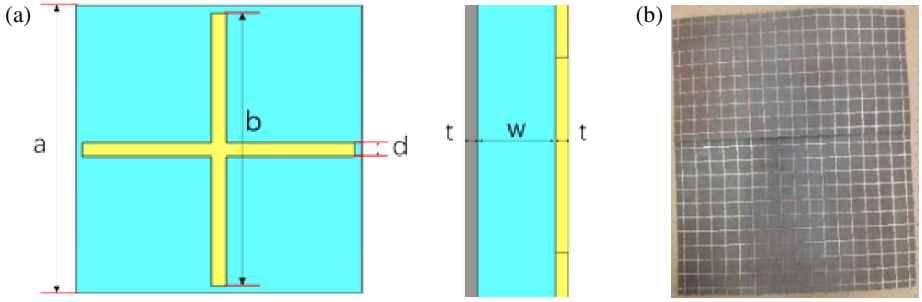

FIGURE 1. (a) Front and side views of the metasurface. (b) Metasurface sample.

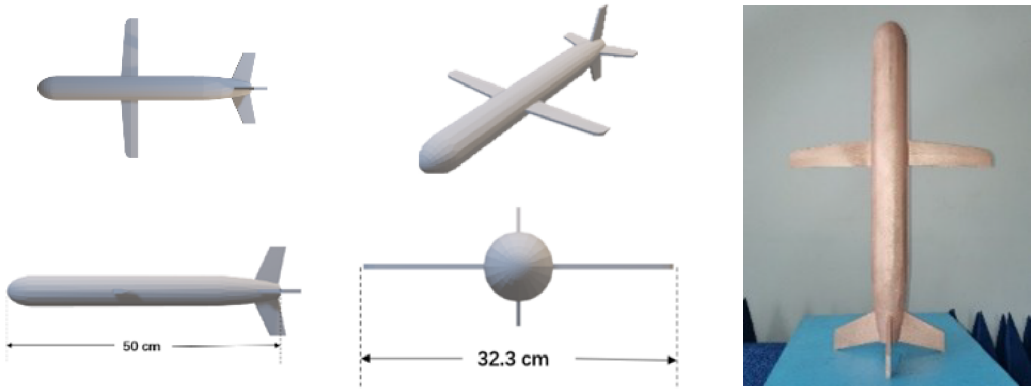

FIGURE 2. Missile 3D model and physical model.

TABLE 1. Metasurface unit design parameters.

Parameter	Description	Value
a	Width of dielectric layer (cell size)	10 mm
b	Length of the cross metal	9.5 mm
d	Width of the cross metal	0.5 mm
w	Thickness of the dielectric layer	0.2 mm
t	Thickness of copper layer and PEC backplane	0.035 mm

under appropriate curvature conditions to maintain stealth characteristics of the coated target. This study used this metasurface to coat a scaled-down missile model and verified the absorption properties of the metasurface through simulation and experiments to support the radar stealth research of targets.

2. SIMULATION AND EXPERIMENT

2.1. Metasurface Design and Target Modeling

This study designed a cross-shaped metal structure metasurface, as shown in Figure 1(a), with the designed parameter values shown in Table 1. With such a geometric parameter design, the metasurface unit can have flexibility, that is, in addition to planes, it can also be coated on cylindrical surfaces with a certain curvature range, making it possible to coat complex models with various types of shapes. The upper layer of the metasurface consists of two mutually perpendicular metal copper strips with the same length and width. The middle layer is a dielectric board made of F4B, with $\varepsilon_r = 2.2$ and $\mu_r = 1$. The bottom perfect electric conductor (PEC) layer is deposited on the dielectric board to eliminate the transmitted wave. The entire experimental sample is made into a 170 mm $\times$ 220 mm array size, as shown in Figure 1(b).

The complex shape used in this study is a missile 3D model as shown in Figure 2, which is generated by 3D printing technology, with a material of resin. The model is 500 mm long, with a wing width of 323 mm and a body radius of 29.5 mm. This size is about 1/8 of the actual shape to meet the laboratory test conditions. The outer layer of the model is evenly coated with conductive copper paint. After testing, the resistance value between the head and tail of the painted model is less than 1 Ω, and the conductivity is good. The model is a combination of various shapes such as planes, cylindrical surfaces, near-spherical

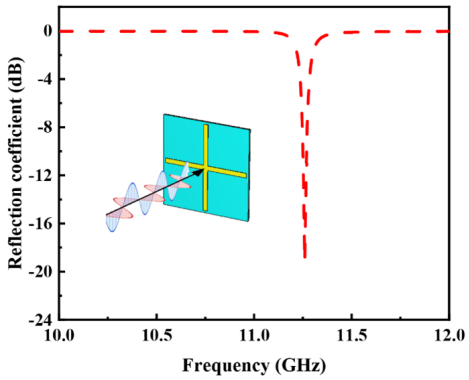

FIGURE 3. Reflection coefficient of the metasurface unit.

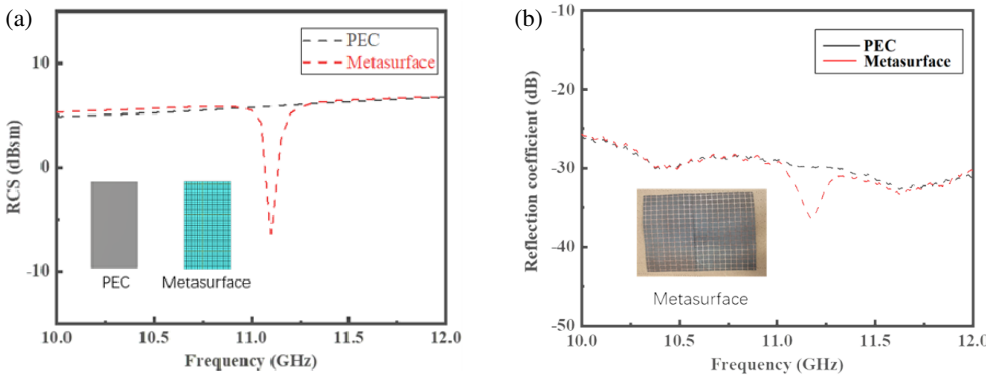

FIGURE 4. RCS comparison of 100 mm × 100 mm PEC and metasurface coating. (a) Simulation. (b) Experimental test.

surfaces, and near-pyramidal shapes, forming various common geometric models in scattering problems. In addition to the aforementioned shapes, the wings of the model also produce a scattering mechanism that is more complex, such as "plane-cylindrical surface-plane" combinations.

2.2. Simulation and Experiment Conditions

The simulation calculation of this study is carried out using the commercial electromagnetic calculation software CST (CST STUDIO SUITE 2022 [37]), setting the boundary conditions, plane wave incidence angles, and working frequency bands that conform to actual application scenarios. The solver used in this study is a time-domain solver, which can use the finite integration technique (FIT). This method discretizes time and space and iteratively calculates the numerical value of the electromagnetic field based on the time-domain form of Maxwell's equations. According to the requirements of this method, the number of grids after the segmentation of pure PEC missile model is about 30 million, and the number of grids after the segmentation of coated missile model is about 200 million. The simulation solution is performed on a computer with a CPU of E5-2620 v4, 4 GeForce 1080Ti GPUs, and 128 Gb of memory. The simulation time for the PEC model is about 20 minutes, and the simulation time for the coated model is about 10 hours and 30 minutes, which will fluctuate with the state of the computer.

Due to experimental conditions, this study uses the difference in scattering coefficients before and after coating as the reduction amount of RCS [35, 36]. The experiment uses an arch frame to test the scattering coefficients.

2.3. Experimental Results and Discussion

First, the metasurface unit is simulated, with the simulation boundary conditions being an infinitely large periodic boundary, and the reflection coefficient of the unit is obtained. The simulation results are shown in Figure 3.

It can be seen from the figure that the metasurface has a strong resonance characteristic near 11.26 GHz, which allows the electromagnetic waves near this frequency to be fully absorbed, and the reflection coefficient reaches −19.19 dB. The metasurface is coated on a 170 mm × 90 mm PEC board, and its far-field RCS simulation is performed. The simulation results are shown in Figure 4(a).

From Figure 4(a), it can be seen that the RCS resonance point of the metasurface is 11.17 GHz, which is about 0.09 GHz shifted compared to the unit simulation, and the reduction amount is about 12.22 dB. Compared with the unit simulation, the reduction amount is reduced by 6.97 dB. One reason is that when the unit simulation is performed, its boundary conditions are infinitely large periodic structures, while when the flat plate is coated with the metasurface for simulation, the boundary conditions are open free space; the number of units is limited; and its edge effects have some impact on the resonance point. Secondly, the meshing accuracy also has a slight impact.

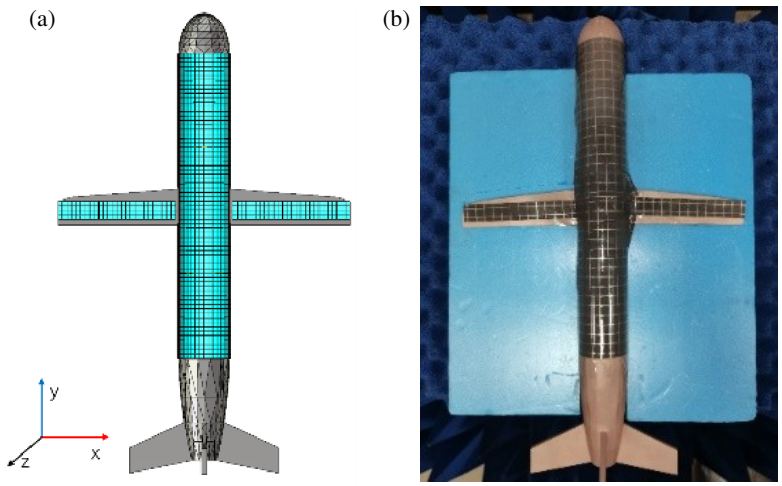

FIGURE 5. Schematic diagram of missile coating method. (a) Simulation. (b) Entity.

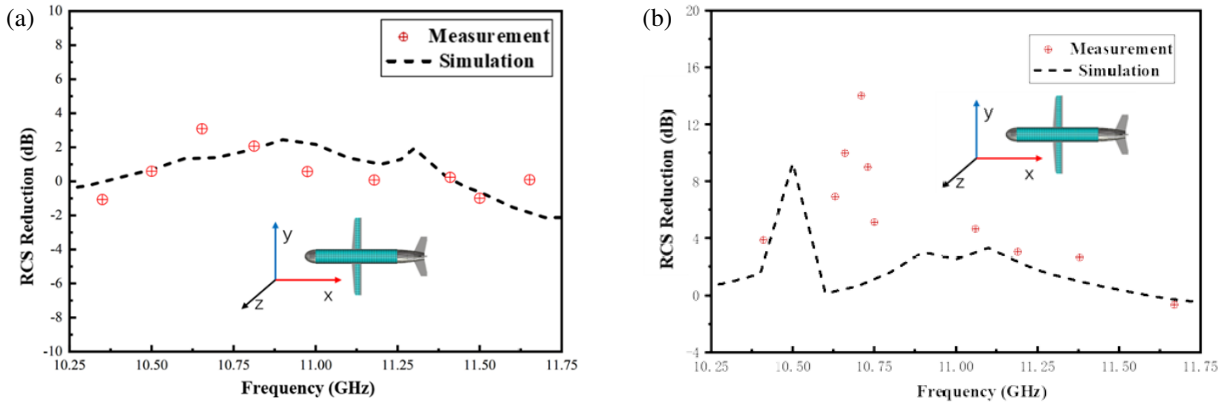

FIGURE 6. RCS reduction amount comparison of missile model. (a) x polarization. (b) y polarization.

The metasurface is fixed in the center of the arch frame, and the center of the receiving antenna and transmitting antenna is aligned with the metasurface entity. The scattering coefficient experimental test results of the 170 mm $\times$ 220 mm metasurface entity are shown in Figure 4(b). The backboard of the metasurface entity is copper. To ensure the same area size, the metasurface is flipped and tested on its back, and the test results were used as the test results of the PEC board. The resonance point of the metasurface test is 11.18 GHz, and the reduction amount compared to PEC is 6.46 dB. The resonance point of this result is almost consistent with the simulation, and the reduction frequency band is slightly widened. There are two main sources of error. The first is systematic error. In the actual measurement process, due to wear and other inevitable reasons, laboratory equipment such as receiving and transmitting antennas and vector network analyzers cannot reach an ideal working state. In addition, the laboratory environment itself is not an ideal vacuum environment, which is also different from the settings of CST simulation software. The second is that the metasurface entity is very thin and easy to form a curved shape, causing the electromagnetic waves to form an oblique incidence on some parts of the metasurface, leading to a slight shift in the resonance point of that part of the metasurface. The combination of all these factors results in a broadening of the band.

To test the RCS reduction effect of the cross-shaped metasurface designed in this study on actual complex models, the metasurface is coated on the bottom of the missile body and the bottom of both wings. The reason for this coating is that in actual applications, the detection waves mainly come from this direction. Due to the limitations of the model's geometric shape and the size of the metasurface itself, the metasurface cannot be exactly and completely coated on both parts of the missile body and wings in the simulation software. To make the coating method more in line with actual requirements and to achieve the best RCS reduction effect, the coating method of the missile model in this study is shown in Figure 5.

In actual coating, the metasurface is made to fit the model as much as possible, and the coating shape is made to be as identical as possible to the simulation. The model with the fitted metasurface is fixed with a foam plate and placed in the center of the arch frame. Due to the volume of the antenna itself, the minimum angle between the transmitting antenna and receiving antenna placed on the arch frame is 10 degrees. The S_{21} at this angle is used to replace the scattering coefficient S_{11}.

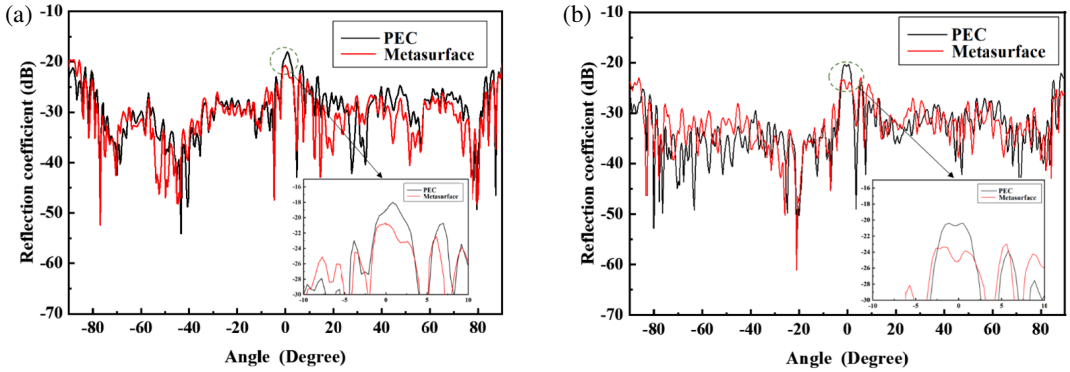

FIGURE 7. Reflection coefficient of the missile. (a) x-polarization. (b) y-polarization.

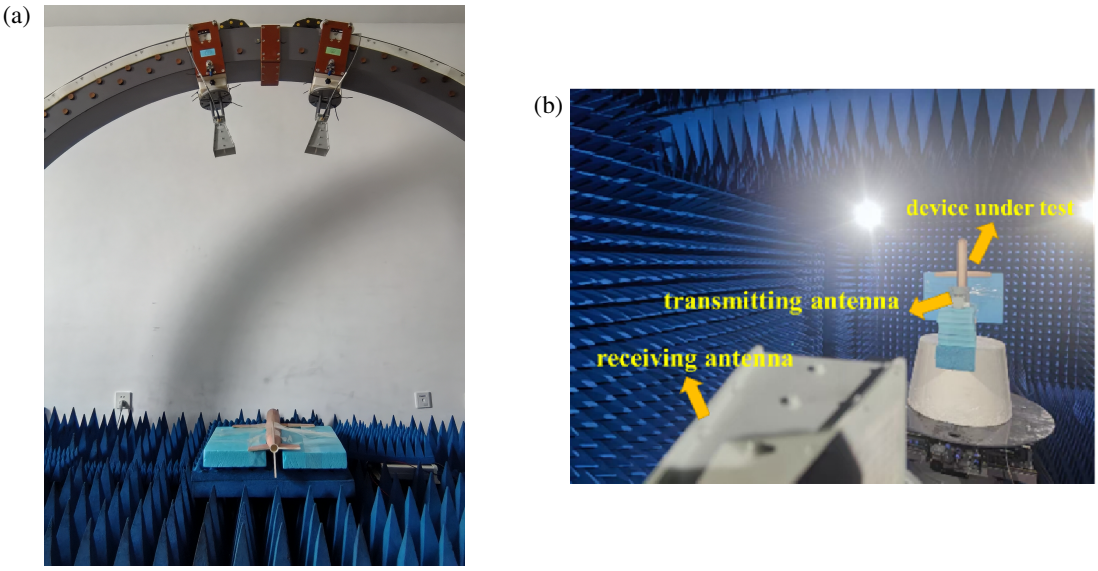

FIGURE 8. Measurement environment for (a) RCS reduction of metasurface and model, (b) microwave anechoic chamber.

The ground around the arch frame is covered with absorbent materials to reduce errors caused by environmental influences. The RCS reduction amount obtained from simulation and experimental tests is shown in Figure 6. It can be seen from the figure that the RCS reduction amount measured in the experiment fluctuates above and below the curve of the simulation results, but the overall trend is consistent. The main sources of error are as follows: Firstly, due to the complexity of the shape, some parts, such as the wings, cannot be completely fitted, resulting in folding, bending, and bulging of some parts of the metasurface. These situations will cause oblique incidence or multiple reflections of the electromagnetic waves on the shape in non-ideal situations. Secondly, the fitting work of the metasurface is completed manually throughout the process, and the position of the fitting is slightly different from that in the simulation. Thirdly, although foam boards and other objects have been used to fix the missile model as much as possible, the experimental environment causes the model's attitude angle and pitch angle to change slightly during measurement, and the electromagnetic waves cannot be exactly facing the missile model as in the simulation.

In a microwave anechoic chamber, the missile model was vertically mounted on a rotating turntable with the transmitting antenna fixed on the same turntable and aligned directly toward the model. As the turntable rotates, the antenna maintains its alignment with the model throughout the movement, enabling the measurement of directional reflection pattern. Experimentally measured reflection coefficients of the missile model are presented in Figure 7. The results demonstrate that for both x-polarization and y-polarization, when the electromagnetic wave illuminates the metasurface-coated side of the missile (corresponding to 0 degrees in the figure), the reflection coefficient shows a 3–5 dB reduction, thereby verifying the RCS reduction effect achieved by the metasurface.

Figure 8 shows the reflection coefficient measurement using an arch fixture and the directional reflection pattern measurement performed in a microwave anechoic chamber.

3. CONCLUSION

This study successfully designed and validated an absorptive metasurface suitable for complex-shaped targets, demonstrating its effectiveness in reducing the radar cross section (RCS).

The metasurface, with a thin design of only 0.27 mm, exhibited strong resonance characteristics near 11.26 GHz, leading to a significant reduction in the far-field RCS of the coated target. The experimental results closely aligned with the simulation findings, confirming the reliability of the metasurface design and its potential application in radar stealth technology.

The flexibility of the metasurface allowed it to be effectively applied to various complex shapes, such as the scaled-down missile model used in this study. This versatility makes it a promising candidate for a wide range of applications, particularly in aerospace fields where stealth capabilities are crucial. The findings of this research not only contribute to the advancement of metasurface technology but also provide a practical solution for enhancing the survivability and operational effectiveness of assets.

Future work could focus on optimizing the metasurface design for broader frequency bands and exploring its integration with other stealth technologies to achieve even greater RCS reduction. Additionally, further experimental validation in more complex and dynamic environments would be beneficial for fully understanding its performance under various operational conditions. Overall, this study lays a solid foundation for the development of advanced radar stealth materials and systems.

ACKNOWLEDGEMENT

This research is supported by the Open Fund Project of Hanjiang National Laboratory (No. KF2024014).

REFERENCES

[1] Chen, H.-T., A. J. Taylor, and N. Yu, "A review of metasurfaces: Physics and applications," *Reports on Progress in Physics*, Vol. 79, No. 7, 076401, Jun. 2016.

[2] Zhang, L., F. Monticone, and O. D. Miller, "All electromagnetic scattering bodies are matrix-valued oscillators," *Nature Communications*, Vol. 14, No. 1, 7724, 2023.

[3] Cui, T. J., S. Zhang, A. Alù, M. Wegener, J. Pendry, J. Luo, Y. Lai, Z. Wang, X. Lin, H. Chen, *et al.*, "Roadmap on electromagnetic metamaterials and metasurfaces," *Journal of Physics: Photonics*, Vol. 6, No. 3, 032502, Jul. 2024.

[4] He, J. and Y. Zhang, "Metasurfaces in terahertz waveband," *Journal of Physics D: Applied Physics*, Vol. 50, No. 46, 464004, Oct. 2017.

[5] Kim, Y. J., J. S. Hwang, Y. J. Yoo, B. X. Khuyen, X. Chen, and Y. Lee, "Triple-band metamaterial absorber based on single resonator," *Current Applied Physics*, Vol. 17, No. 10, 1260–1263, Oct. 2017.

[6] Zhao, Z., X. Li, G. Dong, X. Liu, and X. Mu, "Wideband radar cross-section reduction by a double-layer-plasma-based metasurface," *Plasma Science and Technology*, Vol. 26, No. 6, 065503, 2024.

[7] Guan, J., J.-E. Park, S. Deng, M. J. H. Tan, J. Hu, and T. W. Odom, "Light-matter interactions in hybrid material metasurfaces," *Chemical Reviews*, Vol. 122, No. 19, 15 177–15 203, 2022.

[8] Fang, W., X. Xie, S. Sun, Y. Wang, D. Fan, X. Liu, and P. Chen, "A broadband radar cross section reduction metasurface based on integrated polarization conversion and scattering cancelation," *International Journal of RF and Microwave Computer-Aided Engineering*, Vol. 30, No. 2, e22069, 2020.

[9] Li, Q., J. Zhang, L. Liu, C. He, and W. Zhu, "Graphene-based optically transparent metasurface for microwave and terahertz cross-band stealth utilizing multiple stealth strategies," *Carbon*, Vol. 219, 118833, Feb. 2024.

[10] Sui, S., H. Ma, J. Wang, Y. Pang, M. Feng, Z. Xu, and S. Qu, "Absorptive coding metasurface for further radar cross section reduction," *Journal of Physics D: Applied Physics*, Vol. 51, No. 6, 065603, Jan. 2018.

[11] Zheng, P., Q. Dai, Z. Li, Z. Ye, J. Xiong, H.-C. Liu, G. Zheng, and S. Zhang, "Metasurface-based key for computational imaging encryption," *Science Advances*, Vol. 7, No. 21, eabg0363, 2021.

[12] Wan, S., K. Qu, Y. Shi, Z. Li, Z. Wang, C. Dai, J. Tang, and Z. Li, "Multidimensional encryption by chip-integrated metasurfaces," *ACS Nano*, Vol. 18, No. 28, 18 693–18 700, Jul. 2024.

[13] Watanabe, T., "Image-based radar cross section synthesis for a cluster of multiple static targets," *IEEE Transactions on Instrumentation and Measurement*, Vol. 72, 1–13, 2023.

[14] Fu, H., F. Dai, and L. Hong, "Metasurface aperture design for far-field computational microwave imaging beyond rayleigh diffraction limitations," *IEEE Transactions on Microwave Theory and Techniques*, Vol. 72, No. 1, 223–241, Jan. 2024.

[15] Sun, G., L. Zhu, S. Xing, J. Wang, D. Feng, and X. Wang, "SAR imaging modulation based on time-modulated corner reflector with wide-angle domain control," *IEEE Antennas and Wireless Propagation Letters*, Vol. 22, No. 12, 3157–3161, Dec. 2023.

[16] Lee, J.-I. and D.-W. Seo, "Improvement of computational efficiency for fast ISAR image simulation through nonuniform fast Fourier transform," *IEEE Antennas and Wireless Propagation Letters*, Vol. 20, No. 12, 2402–2406, Dec. 2021.

[17] Pitilakis, A., D. Tyrovolas, P.-V. Mekikis, S. A. Tegos, A. Papadopoulos, A. Tsioliaridou, O. Tsilipakos, D. Manessis, S. Ioannidis, N. V. Kantartzis, I. F. Akyildiz, and C. K. Liaskos, "On the mobility effect in UAV-mounted absorbing metasurfaces: A theoretical and experimental study," *IEEE Access*, Vol. 11, 79 777–79 792, 2023.

[18] Li, L., H. Zhao, C. Liu, L. Li, and T. J. Cui, "Intelligent metasurfaces: Control, communication and computing," *Elight*, Vol. 2, No. 1, 7, 2022.

[19] Brizi, D., N. Fontana, S. Barmada, and A. Monorchio, "An accurate equivalent circuit model of metasurface-based wireless power transfer systems," *IEEE Open Journal of Antennas and Propagation*, Vol. 1, 549–559, 2020.

[20] Shi, H., J. Tian, N. Chen, and W. Zhu, "Wideband high-efficiency scattering reduction in a graphene based optically transparent and flexible metasurface," *Carbon*, Vol. 225, 119150, May 2024.

[21] Shah, M. A., Ç. Tokgöz, and B. A. Salau, "Radar cross section prediction using iterative physical optics with physical theory of diffraction," *IEEE Transactions on Antennas and Propagation*, Vol. 70, No. 6, 4683–4690, Jun. 2022.

[22] Cong, Z., Z. He, and D.-Z. Ding, "RCS calculation of electrically large targets by iterative bidirectionally ray tracing method," *IEEE Antennas and Wireless Propagation Letters*, Vol. 21, No. 12, 2427–2431, Dec. 2022.

[23] Vitucci, E. M., M. Albani, S. Kodra, M. Barbiroli, and V. Degli-Esposti, "An efficient ray-based modeling approach for scattering from reconfigurable intelligent surfaces," *IEEE Transactions on Antennas and Propagation*, Vol. 72, No. 3, 2673–2685, 2024.

[24] Su, D., S. Cui, S. Yang, C. Cao, and Y. Li, "An efficient scheme for quasi-dynamic RCS Estimation of multiple targets based on polarization scattering matrices," *IEEE Antennas and Wireless Propagation Letters*, Vol. 22, No. 12, 3182–3186, Dec. 2023.

[25] Li, S., Z. He, D. Ding, P. Gu, J. Liu, and X. Ai, "Efficient EM scattering analysis of uncertain inhomogeneous medium," *IEEE Antennas and Wireless Propagation Letters*, Vol. 21, No. 6, 1178–1182, Jun. 2022.

[26] Guo, L., D. Xiao, M. Hou, Y. Zuo, and W. Liu, "Fast adaptive modeling of frequency-domain RCS responses by gaussian process regression," *IEEE Antennas and Wireless Propagation Letters*, Vol. 22, No. 12, 3117–3121, Dec. 2023.

[27] He, Z., S.-X. Li, and D.-Z. Ding, "Uncertainty EM scattering prediction for inhomogeneous dielectric bodies of revolution," *IEEE Transactions on Antennas and Propagation*, Vol. 71, No. 1, 882–891, Jan. 2023.

[28] Zhu, F.-Y., S.-R. Chai, Y.-F. Zou, Z.-X. He, and L.-X. Guo, "An efficient and accurate RCS reconstruction technique using adaptive TLS-ESPRIT algorithm," *IEEE Antennas and Wireless Propagation Letters*, Vol. 23, No. 1, 49–53, Jan. 2024.

[29] Shin, H., D. Yoon, D.-Y. Na, and Y. B. Park, "Analysis of radome cross section of an aircraft equipped with a FSS radome," *IEEE Access*, Vol. 10, 33 704–33 712, 2022.

[30] Chai, S.-R., Z.-X. He, P.-K. Dai, F.-Y. Zhu, and Y.-F. Zou, "Research on EM scattering characteristics of targets in land-sea junction area based on the hybrid method of SBR-MECA-PTD," *IEEE Antennas and Wireless Propagation Letters*, Vol. 22, No. 12, 2817–2820, Dec. 2023.

[31] Gao, H.-W., X.-M. Xin, Q. J. Lim, S. Wang, and Z. Peng, "Efficient full-wave simulation of large-scale metasurfaces and metamaterials," *IEEE Transactions on Antennas and Propagation*, Vol. 72, No. 1, 800–811, Jan. 2024.

[32] Cai, Z., M. Hua, W. Gong, and S. He, "An efficient method for analyzing electromagnetic scattering of complex targets coated with anisotropic metal composites," *IEEE Antennas and Wireless Propagation Letters*, Vol. 23, No. 5, 1413–1417, May 2024.

[33] Chen, X., T. M. Grzegorczyk, B.-I. Wu, J. Pacheco, Jr., and J. A. Kong, "Robust method to retrieve the constitutive effective parameters of metamaterials," *Physical Review E*, Vol. 70, No. 1, 016608, 2004.

[34] Epstein, A. and G. V. Eleftheriades, "Huygens' metasurfaces via the equivalence principle: Design and applications," *Journal of the Optical Society of America B*, Vol. 33, No. 2, A31–A50, 2016.

[35] Su, J., W. Li, M. Qu, H. Yu, Z. Li, K. Qi, and H. Yin, "Ultrawideband RCS reduction metasurface based on hybrid mechanism of absorption and phase cancellation," *IEEE Transactions on Antennas and Propagation*, Vol. 70, No. 10, 9415–9424, Oct. 2022.

[36] Jia, Y., Y. Liu, Y. J. Guo, K. Li, and S. Gong, "A dual-patch polarization rotation reflective surface and its application to ultrawideband RCS reduction," *IEEE Transactions on Antennas and Propagation*, Vol. 65, No. 6, 3291–3295, 2017.

[37] CST Studio Suite, "Computer simulation technology AG," Darmstadt, Germany, 2022.